18TH WORLD CONFERENCE ON EARTHQUAKE ENGINEERING
WCEE2024
MILAN

MILAN, ITALY
30TH JUNE - 5TH JULY 2024
www.wcee2024.it

HAUNCH RETROFIT OF RC BEAM-COLUMN JOINT: FASTENING ASSESSMENT

A. Marchisella[1], G. Muciaccia[2]

[1] Department of Civil and Environmental Engineering – Politecnico di Milano, Milano, Italy, angelo.marchisella@polimi.it

[2] Department of Civil and Environmental Engineering – Politecnico di Milano, Milano, Italy

Abstract: *Haunch retrofit of RC beam-column joint is made, essentially, by introducing steel diagonal elements at the beam-column joint location to reduce the shear demand in seismic deficient RC frames. Steel-to-concrete connection is often made using groups of post-installed fasteners, e.g. bonded anchors. This paper addresses the evaluation of anchor's forces using a two-steps structural analysis. First, haunch's diagonal force is evaluated by applying strut-and-tie model to the beam-column sub-assemblage. Second, a FEM model is employed for the sub-structure formed by the steel haunch and anchorages. Validation of both the structural analysis steps is made with respect to experimental results (e.g. measured anchors' forces, reinforcement strains) obtained by the Authors and published elsewhere. Agreement is found when numerically-derived internal forces are compared to experimental ones. Finally, some suggestions are given for practical design cases where estimated forces need to be compared to nominal concrete break-out.*

1. Introduction

Haunch retrofit have been extensively proposed in literature to reduce joint's shear demand in reinforced concrete (RC) moment resisting frames under seismic load. In the recent works, post-installed anchors were used to fasten the metallic haunch to the RC structure and the solution is termed Fully Fastened Haunch Retrofit (FFHR), e.g. Sharma et al. (2014), Genesio, Eligehausen, and Pampanin (2011), Marchisella et al. (2021), Dang and Dinh (2017), Kanchanadevi and Ramajaneyulu (2019). In past research works, haunch was connected to concrete members using collars, e.g. Pampanin, Christopoulos, and Chen (2006), Sharbatdar, Kheyroddin, and Emami (2012). While the latter technique has the advantage of avoiding weakening at the haunch location according to Akbar, Ahmad, and Alam (2020), the issue of invasiveness and practical implementation is higher if compared with FFHR.

In FFHR anchorage to concrete becomes one component in the notorious "ductility chain" according to Paulay and Priestley (1992). In this respect, overstrength should be sufficiently assumed with respect to failure mechanisms characterizing anchorages to concrete as prescribed by EN 1992-4:2018 (2018), e.g. steel breakout, concrete cone, pullout. Nonetheless, the evaluation of forces acting at anchors is not easy-to-handle for a two-fold reason: on one hand, introduction of the haunch in a beam-column joint unit implies statical indeterminacy thus internal forces are dependent on stiffness; on the other, stiffness of the base plate and diagonal might play a role in force distribution as claimed by Bokor, Sharma, and Pregartner (2023).

In this paper, forces at anchorages are derived from sub-modelling a beam-column sub-assemblage as shown in Figure 1. A preliminary strut-and-tie method (STM) application is performed to estimate the axial force acting

at the haunch's diagonal (F_h) for a given value of the beam shear (V_b). Afterward, a finite element (FEM) sub-model is implemented to evaluate the forces acting at anchorages. Such procedure integrates previous practice of RC haunch retrofit. In fact, according to Pampanin, Christopoulos, and Chen (2006) F_h should be evaluated on the basis of β-factor definition. However, according to Marchisella and Muciaccia (2023) STM is more appropriate for haunches characterized by extended base plates. Besides, refined evaluation of anchors' forces have been generally inspired by recent developments addressing the influence of base plate stiffness in anchors' forces distribution, e.g. Bokor, Sharma, and Pregartner (2023), Bokor, Sharma, and Hofmann (2019).

To validate both STM and FEM sub-model, experimentally-derived internal forces were obtained for exterior beam-column joint specimen tested by Marchisella et al. (2021). Test units was exterior beam-column joint with slab and transverse beam. At the end of the test, plastic hinge formed in the beam at drift level larger than 4%. Non-symmetric behavior was recognized generally ascribable to slab participation, i.e. hogging moment capacity of the beam was larger than sagging. Comparison of the internal forces is referred to experimental peak stages.

The paper is structured as follow: (i) in section "Strut-and-tie model" the results of structural analysis using equivalent truss for beam-column joint retrofitted with haunch are presented and discussed with emphasis on shear demand at joint and haunch's diagonal force ; (ii) in section "Haunch FEM sub-model" results using FEM shell model are presented and discussed with emphasis on forces at anchorages; finally some conclusions summarize the work.

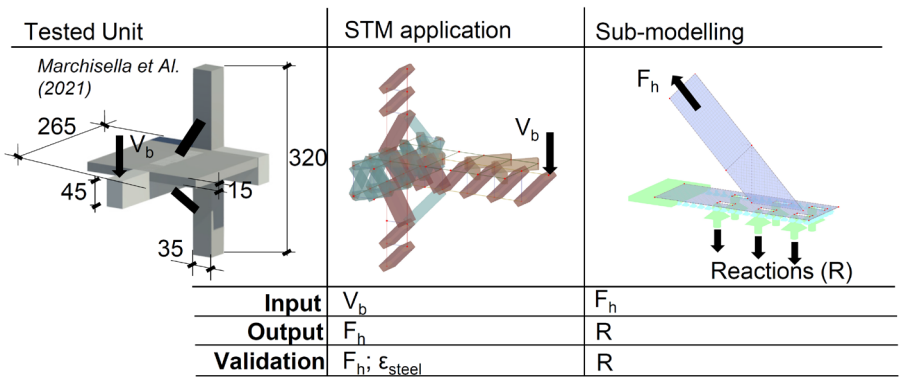

Figure 1: Structural analysis methods used to derive internal forces for beam-column joint. (Notes. Dimensions are given in centimeters.)

2. Strut-and -tie model

Strut-and-tie model (STM) has been applied to exterior joint with slab and transverse beam tested by Marchisella et al. (2021). Essentially, the stress field of sub-assemblage is studied in discrete fashion applying an equivalent truss such as the one shown in Figure 2. The fundamentals of such application, along with its validation, have been presented in Marchisella and Muciaccia (2023) for two-dimensional beam-column joints. In such a case, the hypothesis for structural analysis can be summarized as it follows:

- Concrete can transfer compression (but not tension) only in diagonal direction. The nodes coincide with the intersection between longitudinal and transverse reinforcement.
- Longitudinal reinforcement layers are lumped in an equivalent bar. Two-legs equivalent bar is considered for transverse reinforcement.
- The strut width, of the beam, is assumed equal to eight times the longitudinal bars diameters according to ACI (2021). Same applies for the column.
- The Nodes of the equivalent truss were considered smeared according to Schlaich, Schafer, and Jennewein (1987). Local crushing of concrete has been excluded.
- Materials are considered linear-elastic. A unitary point force is applied at the beam tip, magnified to 100 kN for the sake of a better number representation. Such condition aims at simulating the hogging behavior when the force points downward, sagging behavior for upward direction.

- When the predictions of internal forces are compared with experiments, load stages below the yielding threshold were chosen such that the strains recorded can be converted to stresses using linear stress-strain relation of the steel reinforcement. Such approach was generally inspired by Mitchell et al. (2002).

Additional assumptions have been made to model both the slab and transverse beam. Slab reinforcement in the main beam direction is lumped in a single truss element. The membrane behavior of the slab is modeled connecting longitudinal reinforcement with concrete struts, similarly with what was proposed by Shahrooz and Pantazopoulou (1993). The torsional behavior of the transverse beam is modeled as three-dimensional truss according to Mitchell and Collins (1974). Direction of the strut were suggested by torsional cracks observed experimentally.

Comparison of the presented STM models with respect to experimental results has been carried out considering internal forces essential design variables in haunch retrofit, i.e. shear demand at joint (V_{jh}) and haunch's diagonal force (F_h).

According to Equation (1) V_{jh} is proportional to the force developed at beam's longitudinal reinforcement (either F_{Lb} at bottom layer or F_{Lt} at top) minus shear force at column (V_c).

$$V_{jh} = F_{L,b} - V_c \quad (1)$$

According to Moehle (2015), for typical geometries of un-retrofitted joins the ratio V_{jh}/V_c ranges from 1.5 to 2.5. Moreover V_c always contribute to decrease the magnitude of V_{jh}, thus it is sometimes conservatively neglected. For joints retrofitted with haunches, it can happen that V_c contributes to increase V_{jh} and cannot be neglected in Equation (1). However, in the following validation apply only for F_{Lb} and F_{Lt} which are experimentally-derived from load conversion of strain measured with strain gauge. For example, Figure 3 shows the strain readings and the time chart of the converted load. Similarly, F_h was derived strain gauges glued onto the haunch's diagonal plate.

STM's prediction is made for beam-column sub-assemblage loaded with a force equal to V_b at peak stage of experimental test. Furthermore, comparison with β-factor approach developed by Pampanin, Christopoulos, and Chen (2006) is made as well. Details of β-factor evaluation are reported in Table 1. It is worth mentioning that an average value of β = 2.6 was obtained by considering an equivalent T-shaped beam's cross—section to account for slab's participation. Flexural stiffness of beam was assumed equal to M_y/Φ_y where M_y is the yielding moment of the cross section and Φ_y is the curvature at yielding evaluated according to Panagiotakos and Fardis (2001). Column's deformability was neglected.

Table 2 reports the compared internal forces. Results show that STM predicts conservatively the internal forces both at longitudinal reinforcement and at haunch diagonal. Large differences are recognized for β-factor approach mainly due to the lack of compatibility when using stiff haunches, as claimed by Marchisella and Muciaccia (2023).

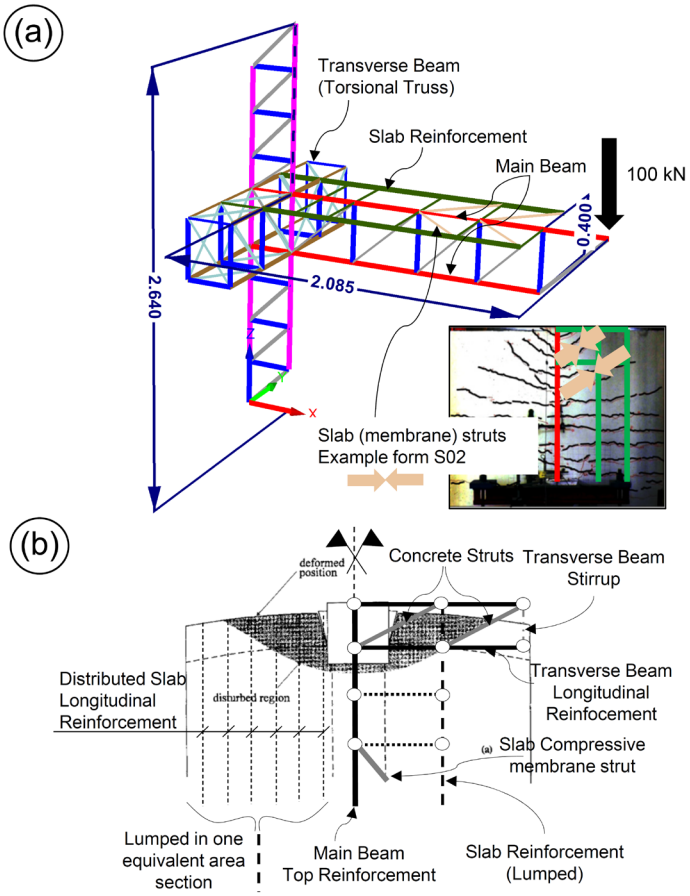

Figure 2. Application of strut-and-tie model for exterior beam-column joint with slab and transverse beam, tested by Marchisella et al. (2021)*: (a) equivalent truss; (b) details of slab's plane modelling. (NOTES. Dimensions are given in meters. Background of (b) is adapted from* Di Franco, Mitchell, and Paultre (2002)*. The Reader is referred to the colour version of this figure.)*

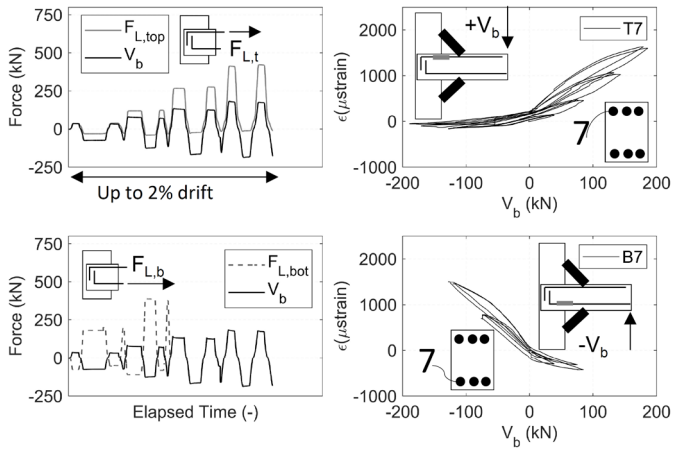

Figure 3. Experimentally-derived forces for longitudinal steel at column-face of beam-column joint tested by Marchisella et al. (2021).

Table 1 β-factor evaluation.

	Hogging		Sagging	
	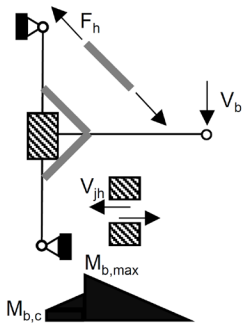		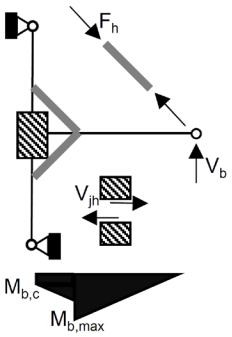	
f_c		31.3		(MPa)
f_y		530		(MPa)
E_c		30978		(MPa)
M_y	469		327	(kN·m)
Φ_y	12		8.9	(rad/km)
EJ_{gross}		8.0E+13		(N·mm)
M_y/Φ_y	3.9E+13		3.7E+13	(N·mm)
β	2.59		2.65	(-)
$M_{b,c}/M_{b,max}$	0.25		0.23	(-)
V_{jh}/V_b	1.48		1.42	(-)
F_h/V_b	0.92		0.94	(-)

Table 2 Comparison between analytically-derived and experimental internal forces for haunch retrofitted beam-column joint specimen tested by Marchisella et al. (2021).(Notes. Values in round brackets are Test-to-predicted ratios)

	HOG			**SAG**		
	V_b (kN)	**F_{Lt}** (kN)	**F_h** (kN)	**V_b** (kN)	**F_{Lb}** (kN)	**F_h** (kN)
Exp.	131	266	NA	164	595	179
β-factor	131	156(1.71)	120(NA)	164	180(3.30)	154(1.16)
STM	131	266(1.01)	166(NA)	164	494(1.21)	210(0.85)

3. Haunch FEM sub-model

A FEM sub-model has been used to study (i) the local stress condition of the haunch plate and (ii) anchors' forces. Numerical results were compared to experimentally-derived ones. For the latter, haunch strains were monitored via strain gauges glued onto the diagonal plate. Anchor forces were monitored via washer load cells. The scheme of the devices used in experimental tests is shown in Figure 4. Only the haunch at the bottom side of the beam was monitored, thus the following discussion refer to sagging behavior, that is when both the haunch diagonal and the anchorages are in tension.

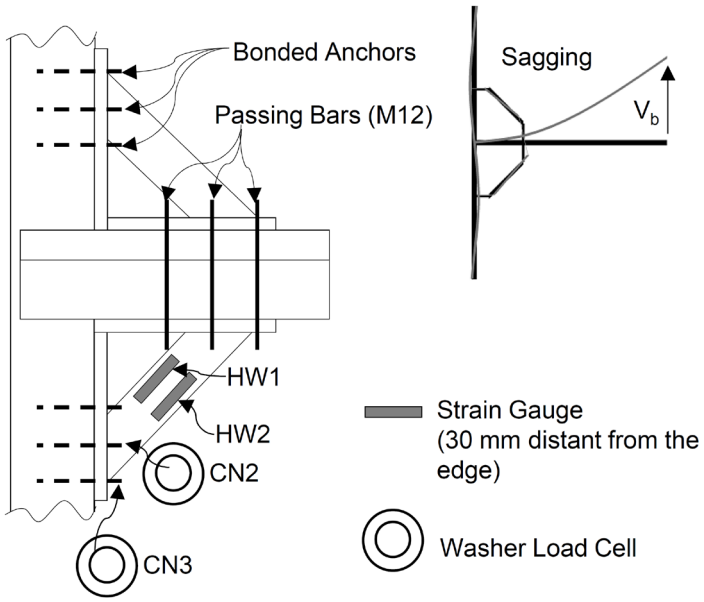

Figure 2. Measuring devices for anchors' forces and haunch's strains.

FEM sub-model was implemented according to the assumptions shown in Figure 5. Specifically, the haunch is isolated from beam column sub-assemblage. The diagonal is assumed to transfer axial force only. The vertical (V) and horizontal (H) base plates are divided at the corner and rigid force transfer is assumed. The free-body equilibrium of V and the attached diagonal (under the N load) requires: (i) anchorages reaction in tension and shear; (ii) friction transfer onto the concrete surface; (iii) force transfer to the base plate H. In the light of kinematic, the isolated plate V and the attached diagonal are fully compatible with concrete sub-grade. Compatibility of the diagonal with plate H is ignored. Moreover, an additional assumption for plate V is made about the concrete sub-grade which is supposed to displace elastically only in the horizontal direction.

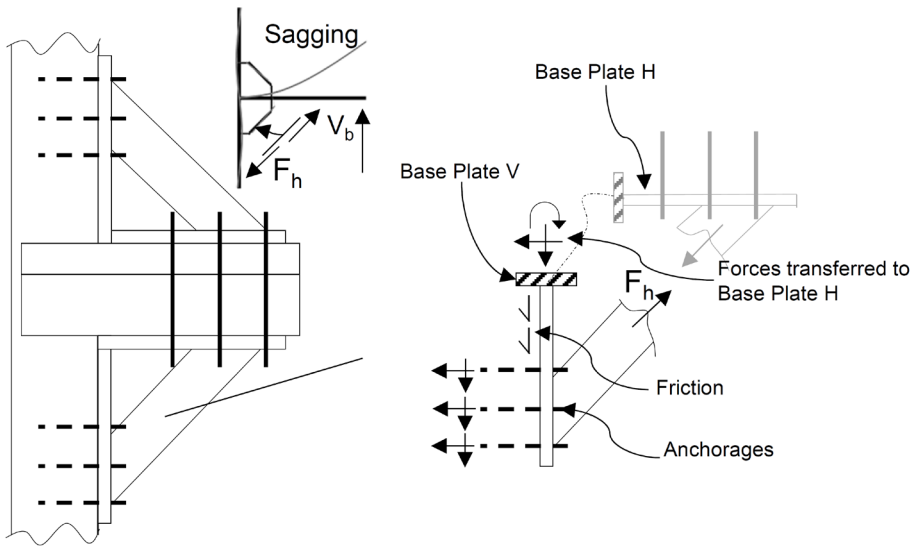

Figure 3. Sub-modelling assumptions.

The FEM model was implemented using commercial FEM software RFEM, distributed by Dlubal (2016). The main features of the model are presented in Figure 6. The base plate V is modelled using shells MITC4 elements, developed by Dvorkin and Bathe (1984). Linear-elastic steel material is assumed for base plate. Same applies to the attached portion of the diagonal plate.

According to Bokor, Sharma, and Hofmann (2019), anchors are modelled as linear elastic springs with axial stiffness (k_a) derived from pullout tests. For all the anchors k_a = 100 kN/mm is assumed without exploring the possible group interaction. It is worth noting that stiffness value is lower with respect to the axial stiffness as it would have been evaluated as a steel rod with length equal to the embedment depth, i.e. E·A/L = 172 kN/mm. Compression-only springs bed is assumed for concrete sub-grade with friction activation. Elastic constant (C in N/mm^3) was equal to 15·f_c according to Li (2017).

Non-Linear static analysis was employed, given the non-linearity of the springfigure bed. Axial force was applied, incrementally, to the diagonal plate as an equally distributed nodal load. The axial force has been derived using STM discussed previously in this paper.

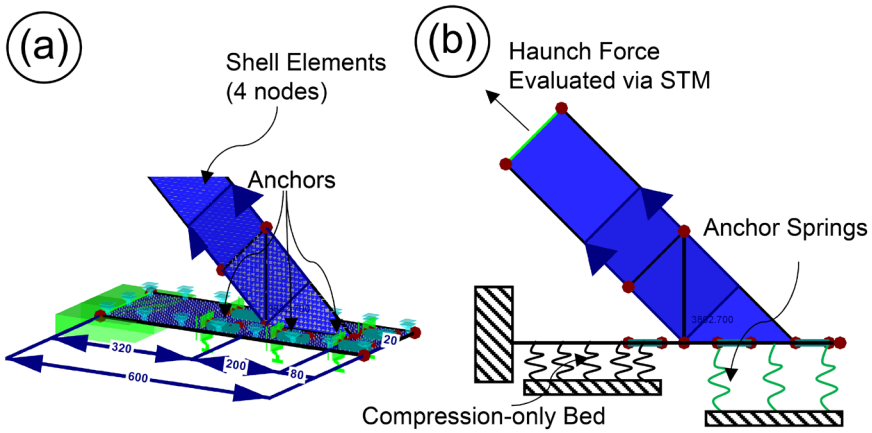

Figure 4. FEM modelling details: (a) model layout; (b) lateral view. (Notes. Dimensions are in millimetres.)

As can be inferred from Figure 7, by assuming the yielding strain of steel approximately equal to 1375 με (f_y / E = 275/200000MPa = 0,001375) it is evident that the haunch's diagonal remains below the yielding threshold thus validating the assumption of elastic material used in FEM. Furthermore, anchors' forces distribution is not regular as it would have been assumed considering a rigid base plate behavior.

Comparison of numerically-derived strains and haunch forces with respect to experimental results is shown in Figure 8. Numerically-derived anchors forces agree to experimental results as V_b increases. The mis-match at low level of V_b is mainly because of pre-load applied to the anchors at the beginning of the experimental test which was loosen progressively. Aside from possible lack of accuracy when strains are computed from displacement-based FEM as remarked by Payen and Bathe (2011), comparison to experimental strains can be sustained if their mean value is considered.

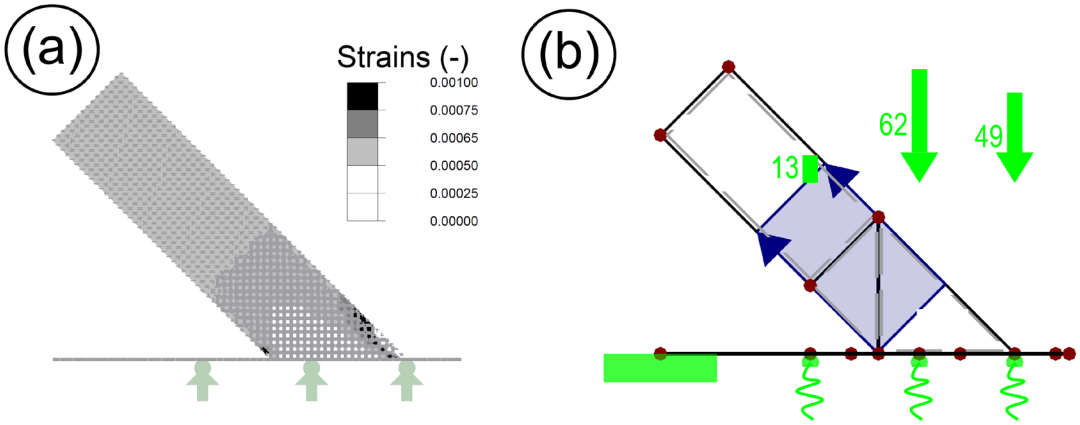

Figure 5. Results of FEM sub-model : (a) diagonal plate's strains; (b) anchorages' forces.

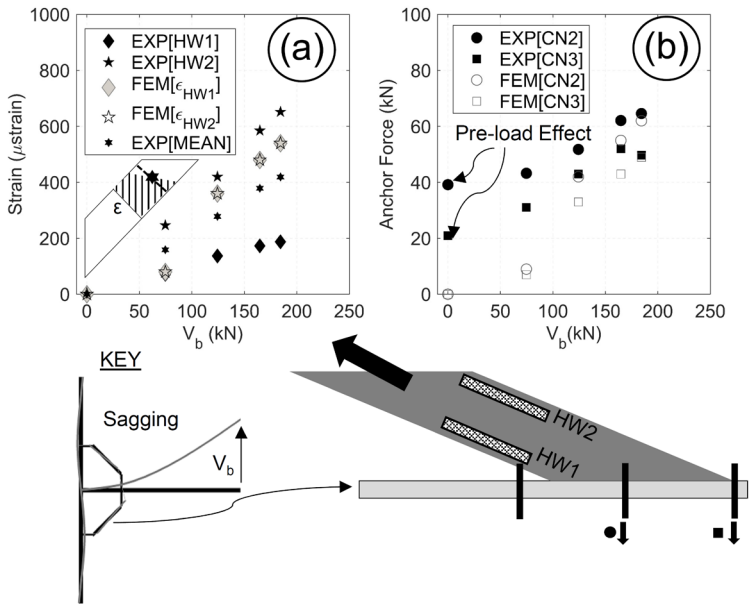

Figure 6. Comparison between FEM and experimental results : (a) diagonal plate's strains; (b) anchorages' forces.

In experimental tests bonded anchors were used at column side whereas passing rods were used for the beam as shown in Figure 9.a. As can be inferred from Figure 9.b (photo was taken at the end of the test), plastic hinge formed in the beam (see the note B1 in the figure). In haunch region flexural cracks were observed for concrete. Nevertheless, anchor failure was prevented. In the following, a comparison between analytically—derived strength and numerical demand at anchorages is presented.

Table 3 presents the results of the estimated load-carrying capacity for the group of six anchors. Both combined pullout and concrete cone (PO+CC) and concrete cone supported by stirrups legs are considered as resistant mechanisms. Strength are evaluated according to EN 1992-4:2018 (2018), by using mean values of the material parameters, such as concrete compressive strength.

The acting force was retrieved from the FEM model previously described. According to Bokor, Sharma, and Pregartner (2023), to apply Concrete-Capacity-Design (CCD, Fuchs, Eligehausen, and Breen (1995))

distribution of forces should be the one obtained by assuming rigid plate assumption. In the presented case, to circumvent the issue the non-uniform distribution of forces was converted to a uniform one with an eccentricity (e) equal to 44 mm as shown in Figure 9.a.

For PO+CC a value of bond strength ($\tau_{max,crack} = 0.5\tau_{max,un\text{-}crack}$) is used, where $\tau_{max,un\text{-}crack}$ is the bond strength, in un-cracked concrete, which is necessary to have concrete-cone mechanism for a single anchor according to Eligehausen, Cook, and Appl (2007). Reduction of fifty percent applies for cracked concrete condition. It is worth to mention that the obtained value is larger than the mean value obtained in seismic crack conditions "C2" according to EOTA (2017) which would have been applied according to recommendations in EN 1992-4:2018 (2018).

Although the group of anchors was not characterized by linear force distribution as it would be necessary according to Bokor, Sharma, and Pregartner (2023), PO+CC strength was based on Concrete-Capacity-Design method according to Fuchs, Eligehausen, and Breen (1995). The analytically-derived strength is less than acting force. The concrete cone resisted by stirrups has a comparable value. However, as previously said, anchor failure was not observed experimentally. Such discrepancy does not belong to the action, which has been validated against experimental reading of anchors' forces. In all the likelihood, resistance underestimation was obtained. For example, the assumed $\tau_{max,crack}$ might have been over-conservative given the moderate crack condition which were observed inside the haunch's region. Yet, although it requires further investigation, the reinforcement might have been active in augmenting PO+CC as claimed by Vita, Sharma, and Hofmann (2022) as much as such anchor resistance might approach the pullout upper bound.

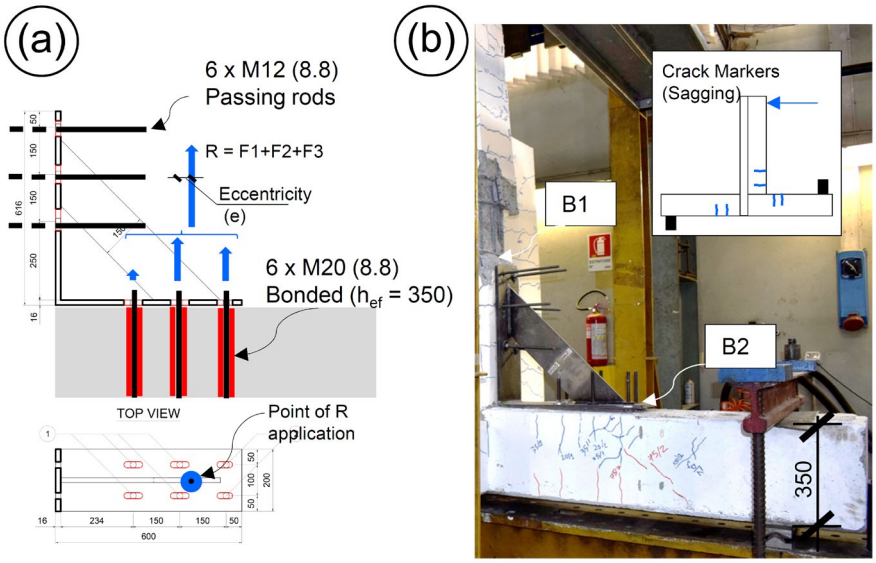

Figure 7. Haunch fastening used in specimen tested by Marchisella et al. (2021)*: (a) layout of the connection; (b) photograph at the end of the test. (Notes. Dimensions are given in millimetres. B1 indicates the plastic hinge formed in the beam. B2 indicates the bonded anchors used for the column. The Reader is referred to the colour version of this figure.)*

Table 3. Assessment of anchorage strength.

Demand			
F_h	248	kN	Derived from FEM model.
Strength			
Combined Pullout - Concrete Cone (according to EN 1992-4:2018 (2018))			
D	20	mm	Diameter
h_{ef}	350	mm	Embedment depth
f_c	30.2	MPa	Cylindrical strength (Mean Value)
$\tau_{max,ucr}$	23.9	MPa	Maximum bond strength – Uncracked according to Eligehausen, Cook, and Appl (2007)
$\tau_{max,cr}$	11.9	MPa	Maximum bond strength – Cracked according to Eligehausen, Cook, and Appl (2007)
τ_{C2}	7.1	MPa	Mean value for C2 seismic according to anchor's European Technical Assessment
$N_{r,g}$	168	kN	Bonded strength – Group of 6 anchors
Concrete cone - Reinforcement (according to EN 1992-4:2018 (2018))			
$N_{r,cc}$	250	kN	Considering 6 stirrups legs activated according to

4. Conclusions

This paper presented an assessment of the anchorage to concrete used in fully-fastened-haunch-retrofit. Anchors' forces were numerically-derived from two-steps structural analysis. Indeed, the haunch force, obtained from strut-and-tie model of the retrofitted beam-column sub-assemblage, was applied to FEM sub-model including steel haunch and anchors. Results of both structural analysis steps were validated against experimentally-derived internal forces of an exterior beam-column joint tested by the Authors.

The outcomes from validation show that strut-and-tie provides reliable estimate of both shear demand at joint and haunch's force. Nonetheless, good agreement was found for anchors' forces numerically-derived from FEM sub-model.

Assessment of anchorage capacity shows that, for bonded anchors, assuming cracked condition for the haunch region might be extremely conservative when anchors are far from plastic hinge region. Besides, activation of reinforcement in enhancing resistance of anchors with respect to combined pullout and concrete cone failure should be investigated further.

5. References

ACI. 2021. "PRC-445.2-21: Strut-and-Tie Method Guidelines for ACI 318-19."

Akbar, Junaid, Naveed Ahmad, and Bashir Alam. 2020. "Response Modification Factor of Haunch Retrofitted Reinforced Concrete Frames." *Journal of Performance of Constructed Facilities* 34 (6): 04020115. https://doi.org/10.1061/(ASCE)CF.1943-5509.0001525.

Bokor, Boglárka, Akanshu Sharma, and Jan Hofmann. 2019. "Spring Modelling Approach for Evaluation and Design of Tension Loaded Anchor Groups in Case of Concrete Cone Failure." *Engineering Structures* 197 (July): 109414. https://doi.org/10.1016/j.engstruct.2019.109414.

Bokor, Boglárka, Akanshu Sharma, and Thilo Pregartner. 2023. "An Assessment Method to Ensure Applicability of Concrete Capacity Method for Design of Anchorages : Linear Force Distribution Approach." *Structural Concrete*, no. March: 1–23. https://doi.org/10.1002/suco.202300255.

Dang, Cong-thuat, and Ngoc-hieu Dinh. 2017. "Experimental Study on Structural Performance of RC Exterior Beam-Column Joints Retrofitted by Steel Jacketing and Haunch." *Advances in Civil Engineering* 2017 (i).

Dlubal. 2016. "Rfem 5 - User Manual."

Dvorkin, Eduardo N., and Klaus Jurgen Bathe. 1984. "A Continuum Mechanics Based Four-Node Element

for General Non-Linear Analysis." *Engineering Computations* 22 (1): 77–88. https://doi.org/10.1108/02644401211227635.

Eligehausen, Rolf, Ronald Cook, and Jörg Appl. 2007. "Behavior and Design of Adhesive Bonded Anchors." *ACI Structural Journal* 104 (5): 645–46.

EN 1992-4:2018. 2018. *Eurocode 2 - Design of Concrete Structures - Part 4: Design of Fastening for Use in Concrete*.

EOTA. 2017. "EAD 330499-00-0601 - Bonded Fasteners For Use in Concrete."

Fuchs, Werner, Rolf Eligehausen, and John Breen. 1995. "Concrete Capacity Design (CCD) Approach for Fastening to Concrete." *ACI Structural Journal* 92 (1): 73–93.

Genesio, Giovacchino, Rolf Eligehausen, and Stefano Pampanin. 2011. "Application of Post-Installed Anchors for Seismic Retrofit of Rc Frames." In *Ninth Pacific Conference on Earthquake Engineering Building an Earthquake-Resilient Society*, 511. Auckland.

Kanchanadevi, A., and K. Ramajaneyulu. 2019. "Non-Invasive Hybrid Retrofit for Seismic Damage Mitigation of Gravity Load Designed Exterior Beam–Column Sub-Assemblage." *Journal of Earthquake Engineering* 0 (00): 1–26. https://doi.org/10.1080/13632469.2019.1592790.

Li, Longfei. 2017. "Required Thickness of Flexurally Rigid Baseplae for Anchor Fastenings." In *High Tech Concrete: Where Technology and Engineering Meet - Proceedings of the 2017 Fib Symposium*. Maastricht.

Marchisella, Angelo, and Giovanni Muciaccia. 2023. "Haunch Retrofit of RC Beam – Column Joints : Linear Stress Field Analysis and Strut-and-Tie Method Application." *Earthquake Engineering and Structural Dynamics* 52 (12): 3575–99. https://doi.org/10.1002/eqe.3921.

Marchisella, Angelo, Giovanni Muciaccia, Akanshu Sharma, and Rolf Eligehausen. 2021. "Experimental Investigation of 3d RC Exterior Joint Retrofitted with FFHR." *Engineering Structures* 239 (July): 112206. https://doi.org/10.1016/j.engstruct.2021.112206.

Mitchell, Denis, and Michael P. Collins. 1974. "Diagonal Compression Field Theory - A Rational Model for Structural Concrete in Pure Torsion." *ACI Journal*, no. 71: 396–408.

Mitchell, Denis, William Cook, Claudia M. Uribe, and Sergio M. Alcocer. 2002. "Experimental Verification of Strut-and-Tie Models." In *ACI SP-208 Examples for the Design of Structural Concrete with Strut-and-Tie Models*, SP-208:41–62. American Concrete Institute.

Moehle, Jack P. 2015. *Seismic Deisgn of RC Buildings*. New York: McGraw-Hill Education. https://doi.org/10.4324/9781315082646-14.

Pampanin, Stefano, Constantin Christopoulos, and Te-Hsiu Chen. 2006. "Development and Validation of a Metallic Haunch Seismic Retrofit Solution for Existing Under-Designed RC Frame Buildings." *Earthquake Engineering and Structural Dynamics* 44 (September): 657–75. https://doi.org/10.1002/eqe.

Panagiotakos, T. B., and Michael N. Fardis. 2001. "Deformation of Reinforced Concrete at Yielding and Ultimate." *ACI Structural Journal* 98 (2): 135–47. https://doi.org/10.14359/10181.

Paulay, Thomas, and Nigel Priestley. 1992. *Seismic Design of Reinforced Concrete and Masonry Buildings*. Wiley.

Payen, Daniel Jose, and Klaus Jürgen Bathe. 2011. "The Use of Nodal Point Forces to Improve Element Stresses." *Computers and Structures* 89 (5–6): 485–95. https://doi.org/10.1016/j.compstruc.2010.12.002.

Schlaich, Jorg, Kurt Schafer, and Mattias Jennewein. 1987. "Toward a Consistent Design of Structural Concrete." *PCI Journal* 32 (May): 74–150. https://doi.org/10.15554/pcij.05011987.74.150.

Shahrooz, Bahram M., and Stavroula Pantazopoulou. 1993. "Modelling Slab Contribution in Frame Connections." *Journal of Structural Engineering (United States)* 118 (9): 2475–94.

Sharbatdar, M., Ali Kheyroddin, and Ebrahim Emami. 2012. "Cyclic Performance of Retrofitted Reinforced Concrete Beam-Column Joints Using Steel Prop." *Construction and Building Materials* 36: 287–94. https://doi.org/10.1016/j.conbuildmat.2012.04.115.

Sharma, Akanshu, G. R. Reddy, Rolf Eligehausen, Giovacchino Genesio, and Stefano Pampanin. 2014. "Seismic Response of Reinforced Concrete Frames with Haunch Retrofit Solution." *ACI Structural*

Journal 111: 1–6. https://doi.org/10.14359/51686625.

Vita, Norbert, Akanshu Sharma, and Jan Hofmann. 2022. “Bonded Anchors with Post-Installed Supplementary Reinforcement under Tension Loading – Experimental Investigations.” *Engineering Structures* 252 (December 2021): 113754. https://doi.org/10.1016/j.engstruct.2021.113754.